10528 *Inorg. Chem.* **2009**, *48*, 10528–10534
DOI: 10.1021/ic900825y

Inorganic Chemistry
Article

Inhibition of Electrocatalytic O_2 Reduction of Functional CcO Models by Competitive, Non-Competitive, and Mixed Inhibitors

James P. Collman,* Abhishek Dey, Christopher J. Barile, Somdatta Ghosh, and Richard A. Decréau

Received April 28, 2009

Electrocatalytic reduction of O_2 by functional cytochrome C Oxidase (CcO) models is studied in the presence of several known inhibitors like CO, N_3^-, CN^-, and NO_2^-. These models successfully reproduce the inhibitions observed in CcO at similar concentrations reported for these inhibitors. Importantly, the data show very different electrochemical responses depending on the nature of the inhibitor, that is, competitive, non-competitive and mixed. Chemical models have been provided for these observed differences in the electrochemical behavior. Using the benchmark electrochemical behaviors for known inhibitors, the inhibition by NO_2^- is investigated. Electrochemical data suggests that NO_2^- acts as a competitive inhibitor at high concentrations. Spectroscopic data suggests that NO released during oxidation of the reduced catalyst in presence of excess NO_2^- is the source of the competitive inhibition by NO_2^-. Presence of the distal Cu_B lowers the inhibitory effect of CN^- and NO_2^-. While for CN^- it weakens its binding affinity to the reduced complex by ~4.5 times, for NO_2^-, it allows regeneration of the active catalyst from a catalytically inactive, air stable ferrous nitrosyl complex via a proposed superoxide mediated pathway.

Introduction

Cytochrome C Oxidase (CcO) is the terminal enzyme in the mitochondrial electron transfer chain that catalyzes the four electron reduction of O_2 to H_2O.[1] In the process it generates a proton gradient across the mitochondrial membrane which is used to drive oxidative phosphorylation. The active site of CcO contains a heme a_3 with a distal Cu_B bound to three histidines, and hence they are often referred to as heme copper oxygenases (Figure 1).[2,3] One of the unique properties of the CcO active site is the presence of a tyrosine residue covalently bound to one of the imidazoles.[4] CcO also contains a heme a and a Cu_A site that are involved in transferring electrons delivered from cytochrome c to the active site. These electrons are derived from metabolism in the form of NADH and are delivered to the heme copper active site via the mitochondrial electron transfer chain. The fully reduced active site binds oxygen and reduces it to H_2O in a multistep redox process involving a few unique intermediates.[1]

Ever since the publication of its crystal structure,[3] there has been an increasing surge of attempts made toward constructing synthetic analogues of this active site that mimic both the structure and the function of this enzyme. Significant contributions have been made by several groups toward the development and use of synthetic inorganic model complexes toward mimicking CcO.[5−7] Over the past several years, a series of functional models have been reported by this lab.[5] These models bear a heme group containing a covalently attached imidazole tail and a distal pocket designed to bind Cu_B.[8] These models successfully reproduce several aspects of the reactivity of CcO, for example, O_2 reduction selectivity, formation of oxy and P_M intermediates (oxoferryl-cupric-tyrosyl radical), and reversible inhibition by NO, and so forth.[9−11] Recently, these complexes were also used to stoichiometrically oxidize reduced cytochrome c using atmospheric O_2.[12]

Electrocatalysis is a powerful tool for analyzing reactivity and kinetics of catalysts under steady state conditions.[13−16]

*To whom correspondence should be addressed. E-mail: jpc@stanford.edu.

(1) Ferguson-Miller, S.; Babcock, G. T. *Chem. Rev.* **1996**, *96*, 2889–2908.
(2) Yoshikawa, S.; Shinzawa-Itoh, K.; Nakashima, R.; Yaono, R.; Yamashita, E.; Inoue, N.; Yao, M.; Fei, M. J.; Libeu, C. P.; Mizushima, T.; Yamaguchi, H.; Tomizaki, T.; Tsukihara, T. *Science* **1998**, *280*, 1723.
(3) Iwata, S.; Ostermeier, C.; Ludwig, B.; Michel, H. *Nature* **1995**, *376*, 660.
(4) McCauley, K. M.; Vrtis, J. M.; Dupont, J.; van der Donk, W. A. *J. Am. Chem. Soc.* **2000**, *122*, 2403–2404.
(5) Collman, J. P.; Boulatov, R.; Sunderland, C. J.; Fu, L. *Chem. Rev.* **2004**, *104*, 561–588.
(6) Eunsuk, K.; Chufán, E. E.; Kaliappan, K.; Karlin, K. D. *Chem. Rev.* (*Washington, DC*) **2004**, *104*, 1077–1134.
(7) Chishiro, T.; Shimazaki, Y.; Tani, F.; Tachi, Y.; Naruta, Y.; Karasawa, S.; Hayami, S.; Maeda, Y. *Angew. Chem., Int. Ed.* **2003**, *42*, 2788–2791.
(8) Collman, J. P.; Fu, L.; Herrmann, P. C.; Zhang, X. *Science* **1997**, *275*, 949–951.
(9) Collman, J. P.; Devaraj, N. K.; Decréau, R. A.; Yang, Y.; Yan, Y. L.; Ebina, W.; Eberspacher, T. A.; Chidsey, C. E. D. *Science* **2007**, *315*, 1565–1568.
(10) Collman, J. P.; Decreau, R. A.; Yan, Y.; Yoon, J.; Solomon, E. I. *J. Am. Chem. Soc.* **2007**, *129*, 5794–5795.
(11) Collman, J. P.; Dey, A.; Decreau, R. A.; Yang, Y.; Hosseini, A.; Solomon, E. I.; Eberspacher, T. A. *Proc. Natl. Acad. Sci. U.S.A.* **2008**, *105*, 9892–9896.
(12) Collman, J. P.; Ghosh, S.; Dey, A.; Decreau, R. A.; Yang, Y. *J. Am. Chem. Soc.* **2009**, *131*, 5034–5035.
(13) Jutand, A. *Chem. Rev.* (*Washington, DC*) **2008**, *108*, 2300–2347.
(14) Saveant, J.-M. *Chem. Rev.* (*Washington, DC*) **2008**, *108*, 2348–2378.
(15) Saveant, J. M. *Acc. Chem. Res.* **1980**, *13*, 323–9.
(16) Cracknell, J. A.; Vincent, K. A.; Armstrong, F. A. *Chem. Rev.* (*Washington, DC*) **2008**, *108*, 2439–2461.

Published on Web 10/14/2009

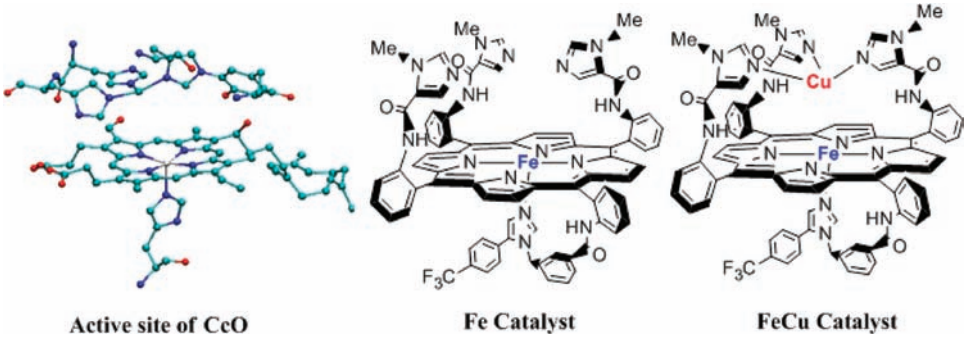

Figure 1. From left, active site of CcO[3], and the Fe[32] and the FeCu[32] catalyst used in this study.

The catalysts are either physi-sorbed on an electrode or covalently attached to a chemically modified electrode. These modified electrodes can then be investigated in aqueous/non-aqueous solvents using rotating disk electrochemistry to obtain steady state kinetic parameters.[17−19] In the past, we have developed and used methods to study the electrocatalytic reduction of O_2 by these catalysts under both slow and fast electron flux.[8,9,20,21] These studies helped understand the details of steady state O_2 reduction by these catalysts under physiological conditions.

Oxygen reduction by CcO is inhibited by small concentrations of several inhibitors.[22] Carbon monoxide (CO), cyanide (CN^-), and azide (N_3^-) are a few common inhibitors that are easily derived from contamination in food and water or during breakdown of amino acids in the body.[22,23] These small ions easily diffuse into the CcO active site and are reported to inhibit CcO at micromolar concentrations. However, these inhibitors affect the kinetics of CcO differently. CO is a competitive inhibitor, that is, it directly competes with O_2 for binding to the active site.[22,24] N_3^- is a non-competitive inhibitor, that is, it does not bind to the active site but binds to some other site and inhibits catalysis via an allosteric effect.[22] CN^- is also reported to be a non-competitive inhibitor although it has been reported to be a good ligand for the reduced active site.[22,25] NO_2^- has been shown to generate NO via its reduction by reduced cytochrome c in the mitochondria.[26] This process has been proposed to deter O_2 consumption during low oxygen concentrations to avoid anoxia.[27] Also, the presence of millimolar concentrations of NO_2^- have been proposed to directly inhibit CcO.[28] Some studies claim that NO_2^- is oxidized to NO_3^- by CcO, while other studies with CcO claim that it is reduced to NO.[28,29] Although there are some reports of inhibitors on enzymes immobilized on graphite electrodes, there are no such reports on inorganic catalysts so far.[30,31]

In this study, we use these Fe-only and FeCu catalysts (Figure 1) immobilized on edge plane graphite (EPG) electrode and study the effect of the presence of inhibitor on their respective O_2 reduction activities. We use ligand binding studies to investigate the role of the distal Cu in ligand binding and correlate them to their respective electrocatalytic behavior.

Experimental Details

Materials and Method. The synthesis of the models are described previously.[32] These models are synthesized in the reduced forms and are as is for spectroscopic measurements. KPF_6, Sodium Azide, Sodium Cyanide, Tetrabutylammonium Cyanide, Cabon Monoxide, Sodium Nitrite were commercial grade and used without further purification. The concentration of CN^- in a pH 7 buffer was corrected for its loss as HCN using the Henderson equation.[33] The CO solutions were made by adding calculated aliquots of saturated CO in deionized water in air saturated buffer solutions. In all cases the system was closed, the head space was minimal, and the experiments were performed with fresh solutions immediately after dissolution.

Rotating Disc Voltammetry. All electrochemical measurements are done at a 100 mM pH = 7 phosphate buffer with 100 mM KPF_6 as the supporting electrolyte. A ring disk assembly with an interchangeable tip (E5 series, Pine instruments) is used for all the linear sweep experiments. The disk assembly is mounted on a rotator shaft which is then connected to a modulated speed rotator (Pine instrument). These experiments were done on a Pine AFCBP1 bipotentiostat using an Ag/AgCl and a Pt mesh as a reference and auxiliary electrodes, respectively.

EPG discs were obtained from Pine Instruments (0.195 cm^2 area). Prior to sample deposition the discs were gently cleaned with 600 grit SiC paper and sonicated in water and ethanol for 30−60 s. A 3−5 μL portion of a 1 mM solution of the catalysts in tetrahydrofuran (THF) or methanol is deposited on these graphite discs, and the solvent is evaporated at room temperature by gently blowing N_2 over it. The catalyst coated disk is sonicated in ethanol for 5 s to remove all unabsorbed/weakly

(17) Shigehara, K.; Anson, F. C. *J. Phys. Chem.* **1982**, *86*, 2776–2783.
(18) Collman, J. P.; Denisevich, P.; Konai, Y.; Marrocco, M.; Koval, C.; Anson, F. C. *J. Am. Chem. Soc.* **1980**, *102*, 6027–6036.
(19) Andrieux, C. P.; Hapiot, P.; Saveant, J. M. *Chem. Rev.* (*Washington, DC*) **1990**, *90*, 723–738.
(20) Collman, J. P.; Devaraj, N. K.; Chidsey, C. E. D. *Langmuir* **2004**, *20*, 1051–1053.
(21) Boulatov, R. C.; James, P.; Shiryaeva, I. M.; Sunderland, C. J. *J. Am. Chem. Soc.* **2002**, *124*, 11923–11935.
(22) Petersen, L. C. *Biochim. Biophys. Acta* **1977**, *460*, 299–307.
(23) Nicholls, P.; Van Buuren, K. J. H.; Van Gelder, B. F. *Biochim. Biophys. Acta, Bioenerg.* **1972**, *275*, 279–287.
(24) Warburg, O. *Biochem. Z.* **1927**, *189*, 354–380.
(25) W. W. Wainio, J. G. *Arch. Biochem. Biophys.* **1960**, *90*, 18–21.
(26) Basu, S.; Azarova, N. A.; Font, M. D.; King, S. B.; Hogg, N.; Gladwin, M. T.; Shiva, S.; Kim-Shapiro, D. B. *J. Biol. Chem.* **2008**, *283*, 32590–32597.
(27) Benamar, A.; Rolletschek, H.; Borisjuk, L.; Avelange-Macherel, M.-H.; Curien, G.; Mostefai, H. A.; Andriantsitohaina, R.; Macherel, D. *Biochim. Biophys. Acta, Bioenerg.* **2008**, *1777*, 1268–1275.
(28) Paitian, N. A.; Markossian, K. A.; Nalbandyan, R. M. *Biochem. Biophys. Res. Commun.* **1985**, *133*, 1104–1111.
(29) Brunori, M.; Forte, E.; Arese, M.; Mastronicola, D.; Giuffre, A.; Sarti, P. *Biochim. Biophys. Acta* **2006**, *1757*, 1144–1154.
(30) Stoytcheva, M. *Electroanalysis* (*New York*) **1995**, *7*, 660–662.
(31) Blanford, C. F.; Foster, C. E.; Heath, R. S.; Armstrong, F. A. *Faraday Discuss.* **2008**, *140*, 319–335.
(32) Collman, J. P.; Sunderland, C. J.; Boulatov, R. *Inorg. Chem.* **2002**, *41*, 2282–2291.
(33) Collman, J. P.; Boulatov, R.; Shiryaeva, I. M.; Sunderland, C. J. *Angew. Chem., Int. Ed.* **2002**, *41*, 4139–4141.

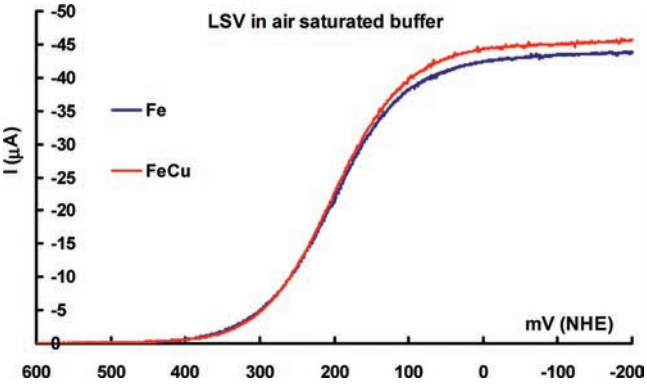

Figure 2. LSV of Fe-only(blue) and FeCu (red) catalysts in air saturated pH 7 buffer. Scan rate 10 mV/s, rotor speed 200 rpm.

absorbed material and blow dried with N_2. This procedure produces most reproducible results.

Measurement of % Catalysis. The % catalytic current is obtained by assuming the current at a certain potential in the absence of any inhibitor as 100% and the background current (measured prior to catalyst deposition) as 0%. The current obtained in the presence of different amounts of inhibitor is normalized using the above scale.

UV−vis. The UV−vis data were collected using a Hewlett-Packard apparatus 8452. Glass cuvette (3 mL capacity) sealed with a 14/24 septum, solvent: THF or 1:1 CH_3CN: pH 7 buffer. Concentration of porphyrin 1×10^{-5} M. The binding constants were evaluated by fitting the binding saturating curves using the "single ligand binding" macro in SigmaPlot.

Electron Paramagnetic Resonance (EPR). EPR spectra were obtained using a Bruker EMX spectrometer, ER 041 XG microwave bridge, and ER 4102ST cavity. All X band EPR samples were run at 77 K in liquid nitrogen finger dewar.

Mass-Spectrometry. Mass spectra were obtained from the Stanford Mass Spectrometry Laboratory. All samples were prepared in an inert atmosphere box and sealed in gastight containers. They were analyzed by loop injection (50 μL/min) on a ThermoFinnigan LCQ ion trap mass spectrometer. The MS was operated in negative and positive ESI modes. The samples had a concentration of 3 mM GSH and were in 1:1 CH_3CN: H_2O.

FTIR. The Fourier transform infrared spectroscopy (FTIR) experiments were performed as described in earlier studies.[34,35] A thin film of the solution was deposited on a KBr palette in a N_2 glovebox, and the solution was evaporated. This film was then sandwiched between two KBr discs and sealed on the outer rim using paraffin film. FTIR data collected using this technique could successfully detect both ferrous and ferric NO species.[35] After data collection, the film was exposed to air to check for oxidative degradation.

Results

1. Electrocatalysis. A typical linear sweep voltammogram (LSV) of these catalysts in air saturated buffer at pH = 7.0 shows electrocatalytic reduction of O_2 (Figure 2) by Fe-only and FeCu catalysts deposited on an EPG disk. Consistent with previous reports, the onset of the catalysis is around 300 mV for these catalysts.[21] The electrocatalytic current increases as the potential is made more negative, until it saturates. At this point the rate is not limited by electron transfer from the electrode but by some other non-redox process (e.g., substrate diffusion). The details of the electrocatalytic behavior of these catalysts have been reported earlier.[21] In this study, we focus on the change of electrocatalytic behavior in presence of known inhibitors of CcO.

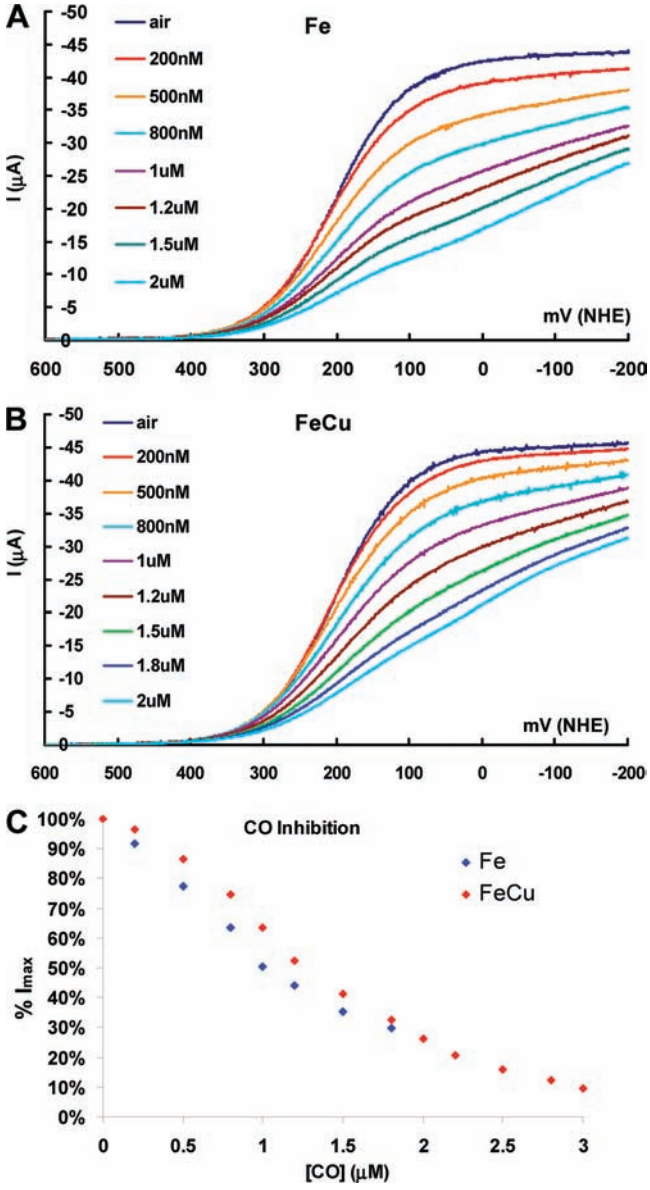

Figure 3. (A) LSV of the Fe-only catalyst in an air saturated buffer with increasing dissolved CO concentration, (B) LSV of the FeCu catalyst in an air saturated buffer with increasing dissolved CO concentration, and (C) plot of catalytic current at +150 mV for Fe-only (blue) and FeCu (red) catalysts at different CO concentrations. The current obtained in an air saturated buffer is normalized to 100% in both cases. Scan speed 10 mV/s, rotor speed 200 rpm.

A. CO. Carbon monoxide is a known competitive inhibitor of CcO.[22] It competes with the substrate (O_2) for binding to the active site. In this case, where the active site can exist in several oxidation states, a competitive inhibitor would specifically bind to the fully reduced $Fe^{II}Cu^{I}$ or mixed valent $Fe^{II}Cu^{II}$ forms of the catalyst as these are the only oxidation states capable of binding, that is, O_2. LSVs of both Fe-only (Figure 3A) and FeCu (Figure 3B) show a steady reduction in O_2 electroreduction

(34) Wasser, I. M.; Huang, H.-w.; Moeenne-Loccoz, P.; Karlin, K. D. *J. Am. Chem. Soc.* **2005**, *127*, 3310–3320.
(35) Collman, J. P.; Yang, Y.; Dey, A.; Decréau, R. A.; Ghosh, S.; Ohta, T.; Solomon, E. I. *Proc. Natl. Acad. Sci. U.S.A.* **2008**, *105*, 15660–15665.

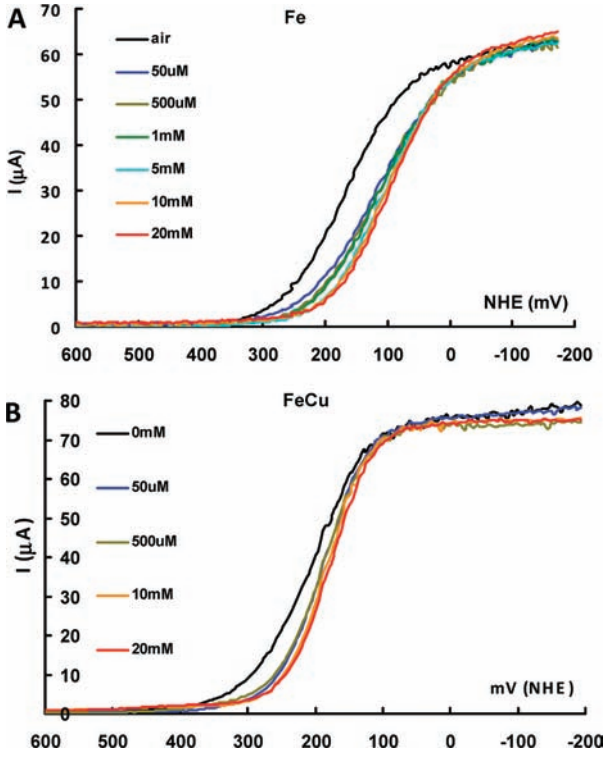

Figure 4. (A) LSV of the Fe-only catalyst in an air saturated buffer with increasing dissolved N_3^- concentration, (B) LSV of the FeCu catalyst in an air saturated buffer with increasing dissolved N_3^- concentration. Scan speed 50 mV/s, rotor speed 200 rpm.

current with increasing concentrations of CO in air saturated buffer. Importantly, there is no shift in the onset of O_2 reduction current in the presence of CO (in buffer). A plot of the catalytic current at 150 mV with increasing concentration of CO indicates that the catalytic current is reduced to 50% in the presence of ~1 μM CO in buffer (Figure 3C). There is no observable difference in the behavior of the Fe-only and FeCu catalyst. O_2 reduction by these catalysts is nearly turned off in the presence of 3 μM CO in buffer.

B. N_3^-. Azide or N_3^- is known to be a non-competitive inhibitor of CcO. LSVs of a Fe-only catalyst in an O_2 saturated buffer at varying concentrations of N_3^- shows that the magnitude of I_{lim} does not change in the presence of N_3^- (in μM-mM range) in buffer (Figure 4A). This implies that the presence of N_3^- does not inhibit steady state O_2 reduction by these catalysts. However, there is an approximate 50 mV negative shift in the onset of the O_2 reduction in the presence of 50 μM N_3^- in buffer (Figure 4A). The FeCu catalyst behaves quite similarly to that of the Fe-only catalyst in the presence of N_3^- in buffer. The catalytic current does not change; however, the potential is shifted more negative by 30 mV (Figure 4B). Thus, the lack of decrease of the steady state O_2 reduction current implies that N_3^- does not competitively bind to the reduced active site of either the Fe-only or FeCu catalysts. However, the potential for catalytic O_2 reduction shifts 30−50 mV negative in the presence of small concentrations of N_3^-. Note that the log plots at the limiting N_3^- concentrations indicate a ~122 ± 5 mV shift in potential per 10-fold increase in catalytic current (i.e., Taffel slope) indicating that the shift in the potential of O_2 reduction possibly has a thermodynamic origin, that is, it reflects the shift of $Fe^{III/II}$ midpoint potential in the presence of N_3^-. Thus, for both Fe-only and FeCu catalysts, N_3^- does not inhibit O_2 reduction. Rather, it lowers the thermodynamic potential for reduction of the oxidized catalyst. Note that this shift is less for the FeCu catalyst relative to the Fe-only catalyst and may indicate lesser stabilization of the individual oxidized metal centers by the bridging N_3^- in the FeCu catalyst relative to the stabilization of the single oxidized metal center in Fe-only catalyst.

C. CN^-. LSVs with small concentrations of CN^- in buffer show that there is a dramatic reduction in the I_{lim} of O_2 reduction as well as a shift of the O_2 reduction to a lower potential for both Fe-only and FeCu catalyst (Figure 5, A, B). The limiting catalytic current is reduced by 90% in the presence of 2 μM CN^- in buffer (Figure 5C). Note that these data also suggest that the presence of the distal Cu reduces CN^- inhibition by almost a factor of 3−5 because it takes 10 μM CN^- to reduce the O_2 reduction current to 10% for the FeCu catalyst relative to 3 μM required for the Fe-only catalyst, and its possible origins are discussed later. Thus, like the competitive inhibitor CO, CN^- causes a clear decrease of steady state O_2 reduction current and like the non-competitive inhibitor N_3^-, CN^- shifts the potential of O_2 reduction more negative for both Fe-only and FeCu catalysts. This shift in potential for O_2 reduction reflects the shifts in thermodynamic reduction potentials reported for these catalysts in anaerobic buffers containing CN^-.[33]

The results presented above using well characterized inhibitors of O_2 reduction provide benchmark parameters that allow testing of other ambiguous inhibitors, for example, NO_2^-.

D. NO_2^-. LSVs in presence of NO_2^- show limited inhibition at low concentrations for both Fe-only and FeCu catalysts (Figure 6 A and B). However, at moderate concentrations (~1 mM), NO_2^- reduces the steady state O_2 reduction current of the Fe-only catalyst by as much as 70% (Figure 6, blue). The change in the LSVs with increasing NO_2^- concentration indicates that NO_2^- is a competitive inhibitor like CO. Interestingly, there is only a modest decrease of the catalytic current in the O_2 reduction current for the FeCu catalyst (Figure 6, red) in the presence of NO_2^- in solution. Thus, inhibition of O_2 reduction by NO_2^- presents an interesting case where the presence of the distal Cu helps resist inhibition by NO_2^-. This may reflect differences in NO_2^- binding affinity between the Fe-only and the FeCu catalyst, or a side reaction of these catalysts with nitrite. These are evaluated below.

2. Ligand Binding Studies. A. CO. CO binds to the reduced Fe^{II} form of these complexes and not to the oxidized form, as reported previously.[25]

B. N_3^-. A detailed recent spectroscopic study using these models indicates that N_3^- binds tightly to the oxidized forms of both the Fe-only and the FeCu complexes in a terminal and a bridging mode, respectively. N_3^- also binds tightly to the mixed valent $Fe^{III}Cu^{I}$ form, where it bridges between the two metals as well.[36] However titration of a solution of the fully reduced catalyst

(36) Collman, J. P.; Dey, A.; Decréau, R. A.; Yang, Y. *Inorg. Chem.* **2008**, *47*, 2916–2918.

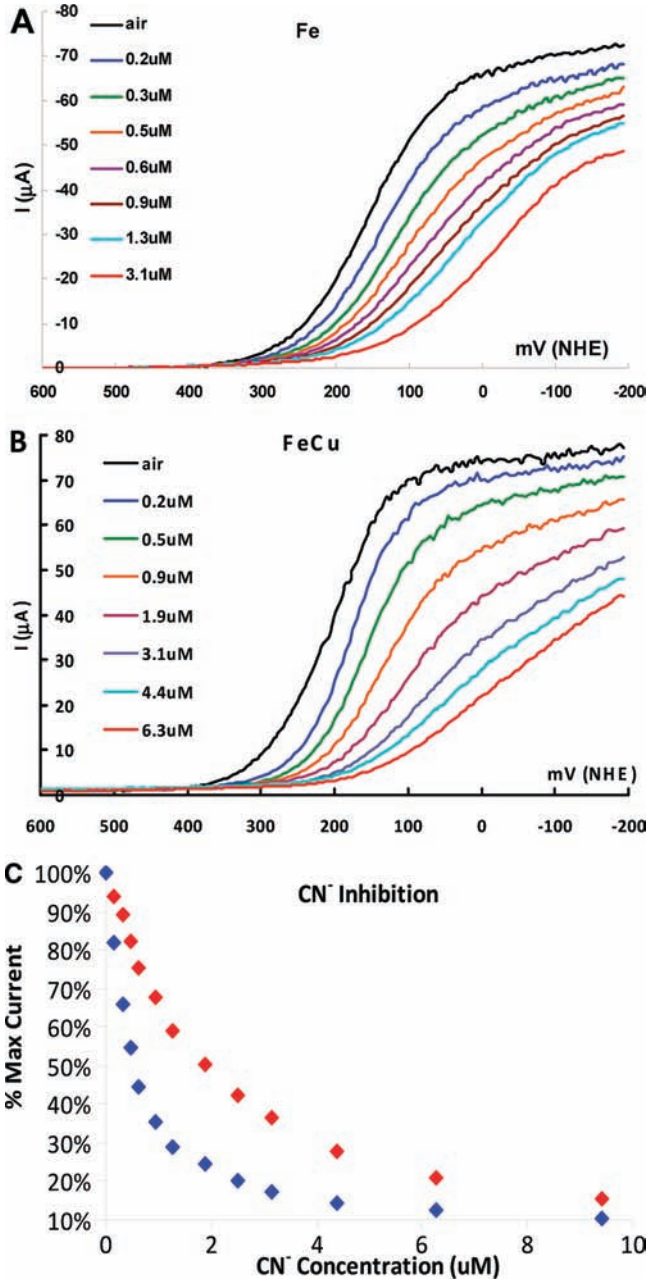

Figure 5. (A) LSV of the Fe-only catalyst in an air saturated buffer with increasing dissolved CN^- concentration, (B) LSV of the FeCu catalyst in an air saturated buffer with increasing dissolved CN^- concentration, and (C) plot of catalytic current at +150 mV for Fe-only(blue) and FeCu (red) catalysts at different CN^- concentrations. The current obtained in air saturated buffer is normalized to 100% in both cases. Scan speed 50 mV/s, rotor speed 200 rpm.

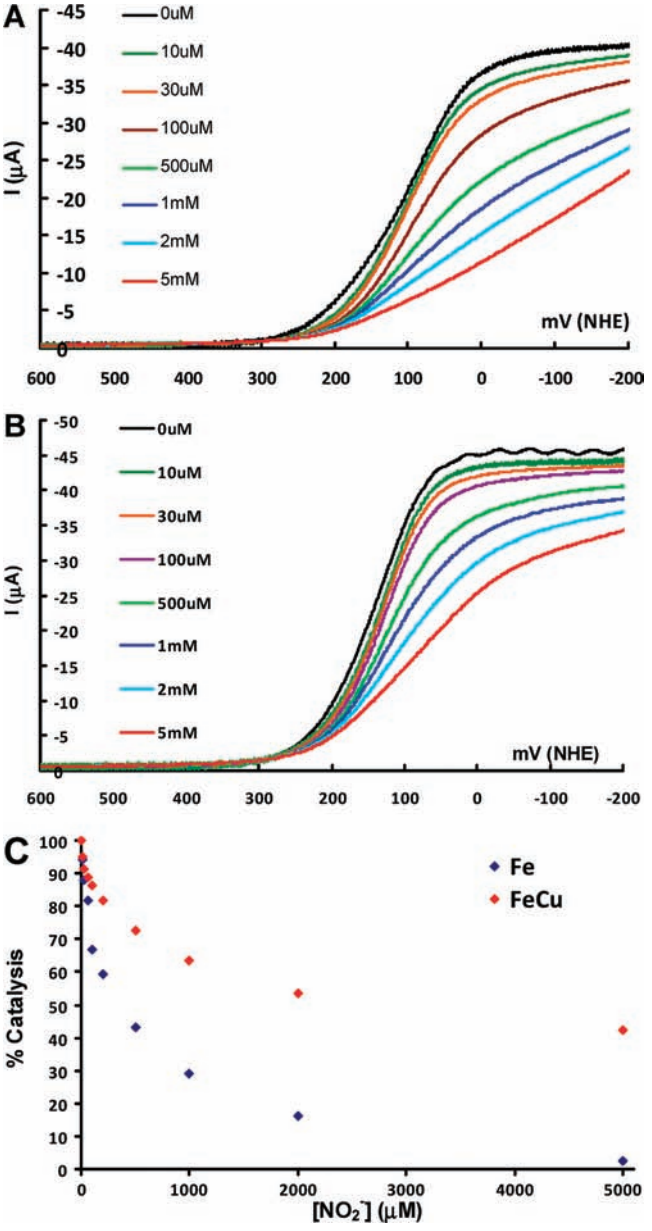

Figure 6. (A) LSV of the Fe-only catalyst in an air saturated buffer with increasing dissolved NO_2^- concentration, (B) LSV of the FeCu catalyst in an air saturated buffer with increasing dissolved NO_2^- concentration, and (C) effect of increasing NO_2^- concentration on Fe-only(blue) and FeCu (red) electrocatalytic reduction current at +150 mV. The catalytic current with air saturated air is normalized to 100% for both catalysts. Scan speed 50 mV/s, rotor speed 200 rpm.

with large excess of N_3^- shows that azide does not bind the reduced metal sites. This is because anionic donor ligands like N_3^- have little affinity for reduced metal centers like Fe^{II} or Cu^{I}.

C. CN^-. Cyanide has been established to bind to the oxidized, mixed valent, and reduced forms of the active site of CcO.[23,37] Titration of the oxidized Fe-only and FeCu complexes indicates quantitative binding with 1 equiv of CN^- (tetrabutylammonium cyanide) consistent with its high binding affinity for the oxidized metal sites.[38] Titration of the reduced Fe-only catalyst with increasing amounts of CN^- (Figure 7, A) shows a single CN^- binding with a K_D of 1.5 ± 0.3 (Supporting Information, Figure S1) (where K_D represents the dissociation constant of the ligand according to the equation; $Fe^{II} + L = Fe^{II}$-L). This reflects a weaker binding of the reduced complex by CN^- relative to that of the oxidized complex. Titration of the reduced FeCu complex with CN^- (Figure 7, B) also indicates a single CN^-binding with a K_D = 5.5 ± 0.5 (Supporting Information, Figure S1), higher relative to

(37) Nicholls, P.; Hildebrandt, V. *Biochim. Biophys. Acta, Bioenerg.* **1978**, *504*, 457–460.

(38) Van Buuren, K. J. H.; Nicholls, P.; Van Gelder, B. F. *Biochim. Biophys. Acta, Bioenerg.* **1972**, *256*, 258–276.

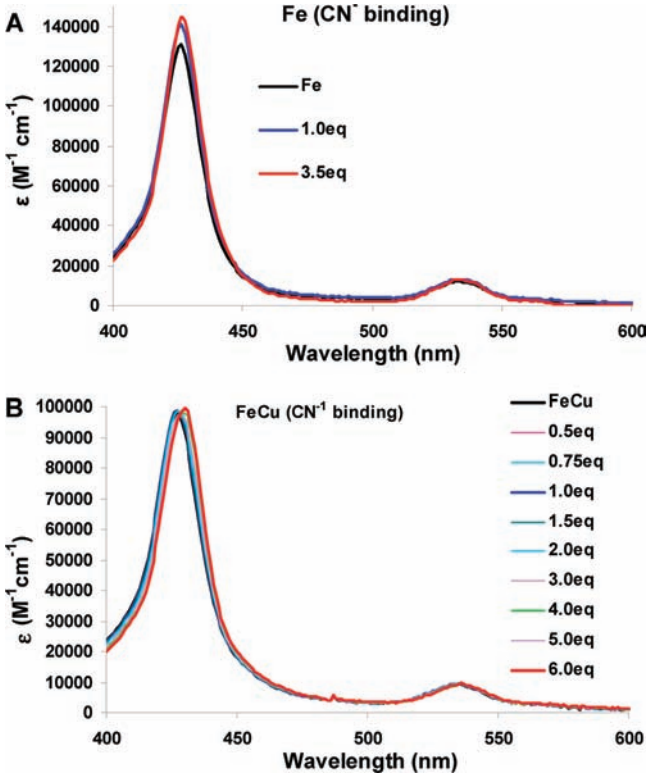

Figure 7. (A) Titration of the reduced Fe-only catalyst with CN^- in THF in absence of O_2. (B) Titration of the reduced CuFe catalyst with CN^- in THF in absence of O_2. The beginning and the end points are indicated by bold black and bold red lines, respectively.

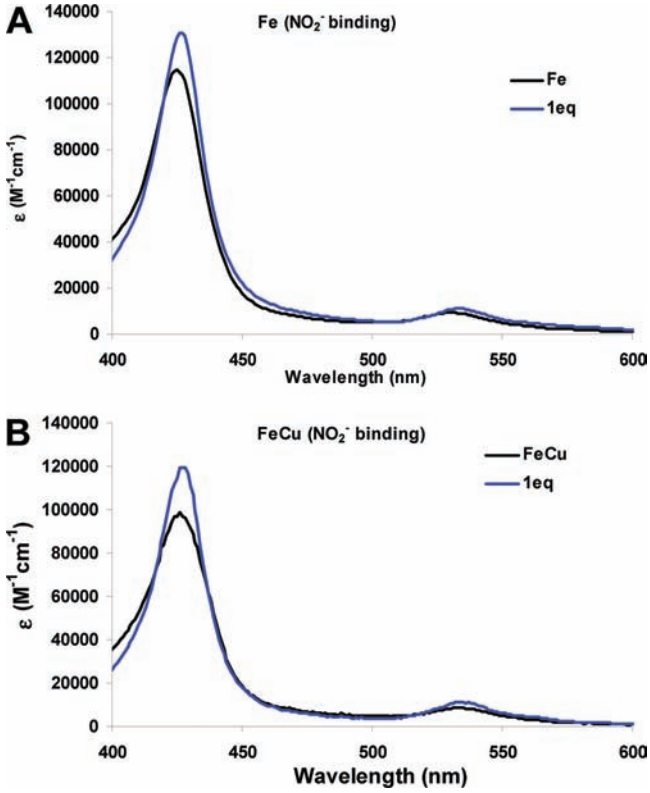

Figure 8. (**A**) Absorption changes associated with NO_2^- binding to the Fe-only catalyst in 1:1 CH_3CN: pH 7 buffer. (**B**) Absorption changes associated with NO_2^- binding to the FeCu catalyst in THF.

that of the Fe-only catalyst. This indicates that the CN^- affinity of the FeCu complex is weaker than that of the CN^- binding to the reduced Fe-only complex by a factor of 4.5. Note that the absolute binding constants will be different in water (electrochemical conditions) but the relative binding constant possibly will not vary significantly. This is indicated by the ~4 times higher CN^- concentrations required to inhibit the FeCu catalyst relative to the Fe-only catalyst.

D. NO_2^-. Addition of 1 equiv of NO_2^- to the oxidized Fe-only and the oxidized FeCu complexes indicates a relatively strong affinity as expected for an anionic ligand. However, titration of the reduced Fe-only and FeCu catalyst with NO_2^- anaerobically also shows a binding step requiring 1 equiv of NO_2^- (Figure 8A and 8B, black to blue). Interestingly, at higher concentrations of NO_2^- (> 1 mM ~ 100 fold excess) it oxidizes the reduced site to generate the oxidized site as indicated by a shift of the Soret band from 428 to 421 nm (data not shown). The NO_2^- on the other hand is reduced to NO. This NO may stay bound to the oxidized Fe^{III} or may be displaced by the excess NO_2^- present in the medium. FTIR of this reaction mixture did not show any heme-Fe^{III}−NO vibration which is generally observed at ~1900 cm^{-1} for six coordinate heme-Fe^{III}−NO complex implying the latter[35,39] However, we trapped the NO released in this reaction via the formation of NO adduct of glutathione (GSNO) which is characterized by its ESI-MS (Supporting Information, Figure S2).

(39) Scheidt, W. R.; Lee, Y. J.; Hatano, K. *J. Am. Chem. Soc.* **2002**, *106*, 3191–3198.

Discussion

Inhibitors are generally categorized in three broad classes, competitive, non-competitive, and mixed, based on their effect on Michaelis−Menten kinetics. The LSVs of the functional models of CcO in air saturated buffer in the presence and absence of well-known inhibitors of CcO help identify typical effects of the different types of inhibitions on the electrocatalytic current.

Competitive. A competitive inhibitor competes with the substrate for binding to the active site of a catalyst. In this case it is the fully reduced Fe-only or FeCu catalysts which bind the substrate O_2. The inhibitor bound catalyst is inactive, and this leads to the reduction of the catalytic current as seen in the case for CO. Thus with increasing amounts of CO in the medium the catalytic current goes down until all the catalyst is inhibited as shown in Figure 3C. It is important to note that there is no shift in the potential of O_2 reduction in case of competitive inhibition.

Non-Competitive. A non-competitive inhibitor is generally thought to inhibit by binding to anywhere other than the active site and induce inhibition via an allosteric effect. The LSVs of these catalyst with N_3^- in solution show that a non-competitive inhibitor does not reduce the catalytic current for O_2 reduction. This is because N_3^- is a very weak ligand for the reduced states that bind the substrate O_2. N_3^- binds to the oxidized (Fe^{III}, $Fe^{III}Cu^{II}$) and the mixed valent ($Fe^{III}Cu^{I}$) forms of the catalyst with high affinity, that is, it requires a stoichiometric amount of N_3^-. This binding, however, shifts the O_2 reduction potential lower by 30−50 mV as an N_3^- binding to the oxidized catalyst makes it is harder to reduce, that is,

the $E°$ for the $Fe^{III/II}$ shifts more negative. A ~200 mV lowering of the $Fe^{III/II}$ potential was reported for N_3^- binding to CcO from bovine heart.[40] While this lowering of potential of O_2 reduction does not affect electrocatalysis as the potential of the electrode can be lowered as well, the same shift of potential in the heme a_3 site in CcO because of N_3^- binding will significantly lower the driving force for electron transfer from the heme a (which is held at a fairly constant potential in the enzyme) to heme a_3. This will inhibit ET between heme a and heme a_3 causing inhibition of O_2 reduction by N_3^-.

Mixed. A mixed inhibitor shows the properties of both a competitive and non-competitive inhibitor. CN^- is a good example of a mixed inhibitor. This is because CN^- binds to the oxidized as well as the reduced catalyst. Thus like a non-competitive inhibitor N_3^-, it shifts the reduction of O_2 to a lower potential by lowering the $E°$ for $Fe^{III/II}$ as it binds to the oxidized site. However, like the competitive inhibitor CO, CN^- also binds to the reduced site and lowers the catalytic current. As discussed in section 2D, CN^- binding to the oxidized catalyst is tighter and requires a stoichiometric amount of CN^- in the buffer whereas the binding to the reduced catalyst is relatively weaker and requires 4−5 times higher concentration of CN^-. This has an interesting effect on the decrease of the catalytic current at different potentials. A plot of the catalytic current at a more oxidizing potential of +220 mV decreases rapidly with increasing CN^- concentration (Figure 9, red) reflecting the lowering of O_2 reduction potential because of CN^- binding. This reflects the non-competitive inhibition of O_2 reduction by CN^- as it binds the Fe^{III} site and shifts the $E°$. Alternatively, the catalytic current at more reducing potential of +50 mV (which is not affected by the shift of $E°$ of $Fe^{III/II}$) reduces less dramatically with increasing CN^- concentration (Figure 9, green) as it reflects the weaker binding affinity of the reduced catalyst which requires higher CN^- concentrations. At these potentials CN^- is acting as a competitive inhibitor where it is competing with O_2 for binding the reduced Fe^{II} active site.

The distal Cu_B metal plays a distinct role in lowering the inhibitory effect of CN^- and NO_2^-. In the case of NO_2^-, the presence of the distal Cu_B significantly lowers the inhibition observed for Fe-only catalyst. Our ligand binding studies indicate that both the Fe-only and the FeCu catalysts bind NO_2^- quantitatively (i.e., $K_D \ll 10^{-2}$), and thus this observed difference in inhibition between the two does not reflect differences in NO_2^- binding. Alternatively, the presence of excess of NO_2^- can oxidize both the Fe-only and the FeCu catalyst to generate NO in situ. NO is a known competitive inhibitor of CcO. The reduced catalyst can reduce NO_2^- to NO as shown by the NO trapping experiment. This NO can bind both the oxidized, Fe^{III}, or reduced, Fe^{II}, forms of the catalyst. While the Fe^{III}−NO complex can be hydrolyzed to regenerate active catalyst, the Fe^{II}−NO complex is inert in oxygenated buffers.[11,41] This can explain the loss

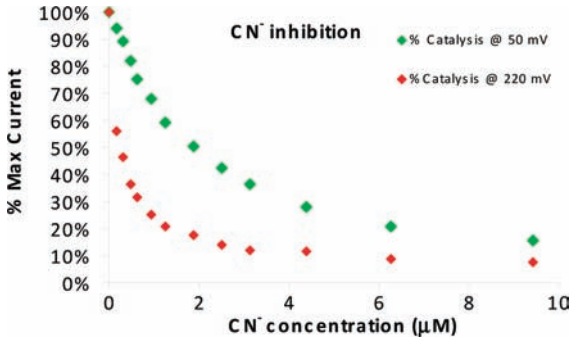

Figure 9

of electrocatalytic activity of the Fe-only catalyst in presence of NO_2^-. It is important to remember that the generation of NO from the reduced catalyst requires excess NO_2^-, and thus the inhibition is observed only at high concentrations. Recently, it was shown that in presence of the distal Cu_B and O_2, this model complex can regenerate the active catalyst after the initial formation of the catalytically inactive Fe-NO complex via a peroxynitrite pathway.[11] EPR data on ZnCu complex clearly indicates that the reduced distal Cu can react with O_2 generating O_2^- and oxidized Cu^{2+} (Supporting Information, Figure S3). It was proposed that the superoxide generated in situ can react with ferrous NO center to regenerate the active ferrous center.[11] The reduced inhibition of O_2 reduction by NO_2^- in the presence of the distal Cu is consistent with that proposal. The distal Cu_B also lowers the CN^- inhibition by a factor of 4−5, that is, it takes 4−5 times more CN^- to inhibit FeCu catalyst than the Fe-only catalyst. Previously it was invoked that this possibly reflects a difference in CN^- binding to the fully reduced catalyst.[33] Indeed the ligand binding studies reflect a weakening of CN^- binding to the FeCu complex by a factor of 4.5 consistent with the inhibition data. We think this difference originates from the steric affect of the distal Cu_B (possibly having a water derived ligand bound in addition to the three imidazoles) which disfavors the formation of a linear Fe-CN unit. This enables the Fe center of the FeCu catalyst to perform O_2 reduction at CN^- concentrations that will inhibit the Fe-only catalyst.[42,43]

Acknowledgment. This research was funded by NIH GM-17880-38. C.B. would like to thank the Stanford University undergraduate Bing fellowship program. Prof. Edward I. Solomon is thanked for the EPR instrument.

Supporting Information Available: The titration data for CN^- binding to the Fe-only and the FeCu catalysts, the EIS-MS data for the NO trap experiment, and the EPR data of the ZnCu complex. This material is available free of charge via the Internet at http://pubs.acs.org.

(40) Kojima, N.; Palmer, G. *J. Biol. Chem.* **1983**, *258*, 14908–14913.
(41) Averill, B. A. *Chem. Rev.* (*Washington, DC*) **1996**, *96*, 2951–2964.
(42) Demaster, E. G.; Quasi, B. J.; Mitchell, R. A. *Biochem. Pharmacol.* **1997**, *53*, 581–585.
(43) Tsikas, D.; Raida, M.; Sandmann, J.; Rossa, S.; Forssmann, W.; Frolich, J. C. *J. Chromatogr. B* **2000**, *742*, 99–108.